Experimental Study of Torrefaction of Camellia Seed Shell for Solid Fuel Production in the Context of a Carbon Neutrality Roadmap

Li Liu,[a] Zheqi Chen,[a] Zhenwei Yu,[b] Xiujuan Zhang,[c,*] Chunjun Li,[d] and Ruihao Sui [b]

Camellia seed shell (CSS) was torrefied at 200, 230, 260, and 290 °C for 30 minutes in a tubular reactor under a nitrogen atmosphere. The effect of temperature on the fuel quality and combustion characteristics of the torrefaction samples was investigated. The pyrolysis characteristics and kinetics of the raw materials at different heating rates were studied. Compared to the raw material, the roasted samples had an increase in the higher heating value (HHV) range of 0.33 to 4.18 MJ/kg, which reached 24.21 MJ/kg at 290 °C. The mass and energy yield ranged from 93.8% to 65.2%. The decrease in energy yield was much higher than the increase in HHV. The enhancement factor and energy yield correlated well (R^2> 0.99). The combustion behavior and kinetics of the torrefaction samples were studied in detail using the First Order Pseudo Bi-component Separate-stage Model (PBSM-O1). From an economic point of view, the best torrefaction temperature for CSS was 260 °C.

DOI: 10.15376/biores.17.3.4055-4068

Keywords: Torrefaction; Camellia seed shell; Higher heating value; Combustion behavior

Contact information: a: Zhejiang Shuren University, Hangzhou, Zhejiang 310015, China; b: College of Mechanical and Electronic Engineering, Shandong Agricultural University, Taian, Shandong 271018, China; c: Zhejiang Tongji Vocational College of Science and Technology, Hangzhou, China; d: College of Food Science and Engineering, Ocean University of China, Qingdao, Shandong, China.
** Corresponding author: zhangxiujuan2015@hotmail.com*

INTRODUCTION

Torrefaction technology is a pretreatment technology for biomass fuels, which has been developed rapidly in recent years (Dai *et al.* 2019; Tian *et al.* 2020; Chen *et al.* 2022). It refers to a thermal conversion technique for heating biomass in the range 200 to 300 °C under atmospheric pressure and inert atmosphere to obtain the solid product of bio-char. This technology removed moisture and some volatiles from the biomass, which significantly increased the calorific value of the torrefaction products (TPs) and effectively improved the mass of the biomass energy.

Meanwhile, torrefaction destroyed the organic molecular structure in the biomass and reduced the volume of the biomass feedstock, which made the biomass material easy to break and grind (Zhang *et al.* 2018a; Sarker *et al.* 2021). In addition, the hydrophobicity of biomass after torrefaction is also enhanced which is conducive to reducing the cost of transportation and storage and is expected to achieve a large-scale commercial circulation of biomass fuels. Therefore, as the main method and way of efficient utilization of biomass, torrefaction technology has broad application prospects.

Camellia is a unique oil plant in China (Zhang *et al.* 2012; Hu 2022). Camellia seeds are mainly used to extract oil after harvesting, and its oil content is 30% to 40%

(Liang *et al.* 2018). Camellia seed shell is the hard outer seed coat of camellia seed. In 2018, the annual production of camellia seed shells in China exceeded one million tons. The mass of the camellia seed shell accounts for about 40% of the total mass. Camellia seed shell is mainly composed of lignocellulose which is difficult to be decomposed by microorganisms (Cheng *et al.* 2018). Lignocellulose accounts for about 31% of the total weight of the camellia seed shell, which can support and protect the cells of the camellia seed shell (Guo *et al.* 2018). In addition to lignocellulose, the camellia seed shell also contains a small amount of saponin, fat, protein, and proanthocyanidins. The treatment method of direct combustion not only has low thermal efficiency but also pollutes the environment. Therefore, the current problem of rational utilization of the camellia seed shell needs to be solved urgently. Camellia seed shell contains a large number of available ingredients. In recent years, research on the utilization of camellia seed shells has been carried out rapidly. However, at present, many technologies for the development of camellia seed shells are at the stage of research and development, and large-scale production has not yet been carried out.

This study took the camellia seed shell (CSS) as the research object. It was torrefied in a tubular reactor at 200, 230, 260, and 290 °C for 30 minutes under a nitrogen atmosphere to prepare torrefaction products. The combustion characteristics, high calorific value, and functional groups of the samples were analyzed by synchronous thermogravimetric analyzer, elemental analyzer, and Fourier infrared spectrometer. The pyrolysis characteristics and kinetics of the raw materials at different heating rates were studied. The kinetics of the torrefaction samples was studied in detail using the First Order Pseudo Bi-component Separate-stage Model (PBSM-O1) to determine the kinetic parameters. The results will provide a theoretical basis and reference for the resource utilization and harmless utilization of CSS.

EXPERIMENTAL

Materials

In this study, the camellia seed shell was selected as the raw material from local camellia processing plants (Hunan Province, China). The raw materials were dried in an oven at 80 °C for 24 h. Then, the samples were powdered and sieved using a 60-mesh screen, whereby particles with sizes smaller than 212 μm were collected for subsequent torrefaction operation and analysis.

Experimental Apparatus and Procedure

Four different torrefaction temperatures of 200, 230, 260, and 290 °C, regarded as the light (200 and 230 °C), mild (260 °C), and severe torrefaction (290 °C), were used, respectively. In each experiment, the sample (6 ± 0.01 g) was loaded into the quartz boat and placed in the unheated area of the quartz tube. By adjusting the nitrogen control device, the nitrogen flow rate could be controlled at 160 mL/min until the tube furnace was cooled to ensure that the system was always in an inert atmosphere. After the reactor was swept for 5 min, the pyrolysis reactor was heated to the specified temperature at a heating rate of 10 °C/min, and the quartz boat was quickly pushed to the middle of the quartz tube. After maintaining the required time, the quartz boat was pulled to the unheated area of the quartz tube. After the tube furnace was cooled to room temperature, the solid product was collected and weighed for subsequent analysis. The TPs were named according to

temperature, such as the obtained products at 200, 230, 260, and 290 °C were named CSS200, CSS230, CSS260, and CSS290, respectively.

Methods

Chemical analysis

The contents of C, N, H, and S in the raw materials and TPs were measured by using an elemental analyzer (ElementarVario MACRO Cube, Germany), and the content of O was calculated by difference. According to the guidance of the national standard (GB/T28731-2012, Proximate analysis of solid biofuels), the volatile matter and moisture content of various raw materials were monitored. The functional groups of the samples were analyzed using a Fourier transform infrared spectrometer (Thermo Scientific Nicolet iS50, USA). All spectroscopy recorded in the wavenumber ranged from 400 to 4000 cm^{-1} at a resolution of 4 cm^{-1}. The sample was mixed with KBr at the mass ratio of 1:100. It was ground and pressed for infrared spectrometric determination. A synchronous thermal analyzer (NETZSCH STA 449F3, Germany) was used to measure the combustion characteristics of samples. The 10 mg sample was heated to 800 °C at a heating rate of 20 °C/min with an airflow of 100 mL/min. The role of air is to provide a reaction atmosphere for the combustion reaction to ensure that the raw materials can be fully burned under the condition of sufficient oxygen. Meanwhile, the volatile products produced by the sample in the furnace were promptly taken away, to avoid the influence of secondary reactions on the instantaneous mass of the sample as far as possible.

In this study, the used measure of calorific value was the higher heating value (Huang *et al.* 2017). In this paper, the fitting algorithm proposed by Friedl's team (Friedl *et al.* 2005) for calculating the high calorific value of biomass was used to determine the high calorific value of raw materials before and after torrefaction. The calculation formula was as follows:

$$\mathrm{HHV} = 3.55\,C^2 - 232C - 2230H + 51.2C \times H + 131N + 20600 \quad (1)$$

Mass and energy yields and energy densification ratio are important indicators for biomass torrefaction, because they help observe the transition and densification of mass and energy from raw feedstock to torrefied biomass. The mass and energy yields show the overall mass and energy ratios of a torrefaction product to its original biomass feedstock. The enhancement factor reflected both energy output and energy densification of the obtained biochar. Mass yield and energy yield are important methods for studying torrefaction output and measuring torrefaction efficiency (Xin *et al.* 2018). The mass yield, energy yield, and enhancement factor after torrefaction were calculated according to the following formulas (Gucho *et al.* 2015).

$$Massyield(\%) = \frac{m_i}{m_0} \times 100 \quad (2)$$

$$Enhancement\ factor = \frac{HHV_i}{HHV_0} \times 100 \quad (3)$$

$$Energyyield = \frac{m_i \times HHV_i}{m_0 \times HHV_0} \times 100 = Massyield \times Enhancement\ factor \quad (4)$$

where m_0 is the mass of the material before torrefaction (g), m_i is the mass of the material after torrefaction (g), HHV_0 is the high calorific value of the material before torrefaction (MJ/kg), and HHV_i is the high calorific value of the material after torrefaction (MJ/kg).

Combustion Kinetic Analysis

As part of chemical kinetics, combustion kinetics studies the general laws of chemical kinetics. The chemical reaction plays an important role in the combustion process, which controls combustion phenomena such as ignition, flameout, combustion stability, and pollutant emission. In order to better study the complex chemical reactions in the combustion process, combustion kinetics was developed. The kinetic parameters, activation energy, and pre-exponential factor of the samples combustion were determined by the integral method (Chen and Bach 2017; Mehmood *et al.* 2017). It is assumed that solid fuel combustion is a first-order reaction. So the samples combustion reaction equation may simply be expressed as the following formula,

$$x = \frac{W_0 - W_t}{W_0 - W_f} \quad (5)$$

$$\frac{d_x}{d_t} = Aexp\left(-\frac{E}{RT}\right)(1-x) \quad (6)$$

where W_0 is the original mass of the test sample; W_t is the mass at time t, and W_f is final mass at the end of pyrolysis. The parameter A is the pre-exponential factor, E is activation energy, T is temperature, and t is time.

For a constant heating rate H during combustion, H=dT/dt, rearranging Eq. 6 and integrating gives:

$$ln\left(\frac{-ln(1-x)}{T^2}\right) = \left(\frac{AR}{HE}\left(1-\frac{2RT}{E}\right)\right) - \frac{E}{RT} \quad (7)$$

Assuming that the combustion is a first-order reaction, a straight line can be obtained by plotting ln[-ln(1-x)/T^2] and 1/T. The activation energy can be determined from the slope of the line. By taking the temperature at which W_t=(W_0+W_f)/2 in place of T in the intercept term of Eq. 7, the pre-exponential factor can also be determined.

RESULTS AND DISCUSSION

Ultimate Analysis

The ultimate analysis of the samples under different torrefaction conditions and the calorific values are shown in Table 1. When the torrefaction temperatures were 200, 230, 260, and 290 °C, the increase of carbon contents in the TPs was 0.88%, 1.88%, 6.69%, and 10.11%, respectively. This phenomenon was caused by the evaporation of volatile matter (when the baking temperature was 200, 230, 260, and 290 °C, respectively, the content of volatile matter in TPs is 68.47%, 62.28%, 56.72%, and 49.13%, respectively.) from the sample during the torrefaction process, which led to a significant reduction in the mass of the sample. However, the total amount of fixed carbon in the sample changed little; therefore, the fixed carbon contents of the TPs were higher than those of the raw materials. Although volatile carbon was lost as volatile matter when being heated, which reduced the total amount of carbon elements in the product, the contents of these carbon elements were less, thus the influences were limited. The relative content loss rate of volatile carbon was much lower than the relative content growth rate of fixed carbon, so the relative content of carbon in the TPs after torrefaction was different from the non-torrefied sample in terms of the overall ratio. Compared with the raw materials, as torrefaction temperature was increased, the torrefaction degree of samples became deeper, and accordingly the carbon

content of the sample was higher. Meanwhile, carbon is the main source of biomass calorific value, so the calorific value of TPs will increase significantly.

The content of hydrogen in the raw material was only 5.94%. This hydrogen element was present in the raw material, mainly in the form of H_2O or hydrocarbons, by combining with oxygen or carbon elements. The roasting process was accompanied by decarboxylation and dehydration reactions. The reaction became more intense with the increase of baking temperature, resulting in more desorption of hydrogen. Simultaneously, the decrease in hydrogen content can be explained by loss of hydrogen through release of H_2O. Oxygen was the most sensitive to temperature change, as it was released as CO_2, CO and O_2, whereas hydrogen was only released as H_2O. During the torrefaction process, the free water and the bound water were evaporated by heating, and the hemicelluloses were thermally decomposed into gaseous substances. Therefore, compared with the raw materials, it can be seen from the table that the hydrogen content of the TPs was lower. However, the reduction magnitude was minor, no more than 1%.

The content of the oxygen element in the sample was generally higher, only lower than the carbon element. As shown in Table 1, when the torrefaction temperatures were 200, 230, 260, and 290 °C, the contents of the oxygen element in the TPs decreased by 0.73%, 1.7%, 6.26%, and 9.84%, respectively. The reduction of oxygen content in TPs was very similar to that of carbon. The reduction was more pronounced as the torrefaction temperature increased, which can be attributed to the evaporation and precipitation of free water and bound water consisting of oxygen elements during torrefaction. Meanwhile, owing to the decarboxylation and hydroxyl reaction of raw materials in the process of torrefaction, some cellulose and hemicellulose were decomposed into H_2O, CO_2, CO, and carbohydrate released in the form of volatile compounds, which decreased the content of oxygen in TPs significantly.

Table 1. Ultimate Analysis of Samples at Different Torrefaction Temperatures

Biomass	Ultimate analysis, wt%				
	CSS	CSS200	CSS230	CSS260	CSS290
C	50.36	51.24	52.24	57.05	60.47
H	5.94	5.79	5.78	5.48	5.31
N	0.33	0.34	0.32	0.37	0.46
S	0.09	0.08	0.08	0.08	0.32
O	43.28	42.55	41.58	37.02	33.44
HHV, (MJ/kg)	20.03	20.36	20.78	22.75	24.21

Mass and Energy Yields

As mentioned earlier, mass yield, enhancement factor and energy yield are important indicators that are used for the evaluation of torrefaction performance. The mass yield is used to evaluate the influence of torrefaction on the mass loss, which often corresponds to the energy yield. The enhancement factor reflects both energy output and energy densification of the obtained biochar. The mass yield, energy yield, and enhancement factors of TPs at different temperatures are shown in Fig. 1. As shown, the mass yield decreased with the increase of torrefaction temperature. When the torrefaction temperature was below 230 °C, the mass yield decreased slowly; when the torrefaction temperature was raised from 230 to 290 °C, the mass yield of the sample significantly reduced from 93.83% to 65.22%, and the decline rate remained stable. The torrefaction temperatures were 230, 260, and 290 °C, the decline rates of the mass yield of the samples

were 0.21%/°C, 0.38%/°C, and 0.39%/°C, respectively. The mass loss in the early stage was mainly due to the loss of bound water and the decomposition of aliphatic compounds. Due to there being more depolymerization and depolymerization reactions, the mass dropped sharply when the temperature rose to 230 °C. During the process from 230 to 290 °C, aliphatic and aromatic compounds in carbohydrate and protein structures, as well as hemicellulose and cellulose, continued to undergo thermal decomposition. These substances depolymerized and recombined by the loss of CO_2, CO, and H_2O, which led to the formation of stronger bonds between carbon and carbon.

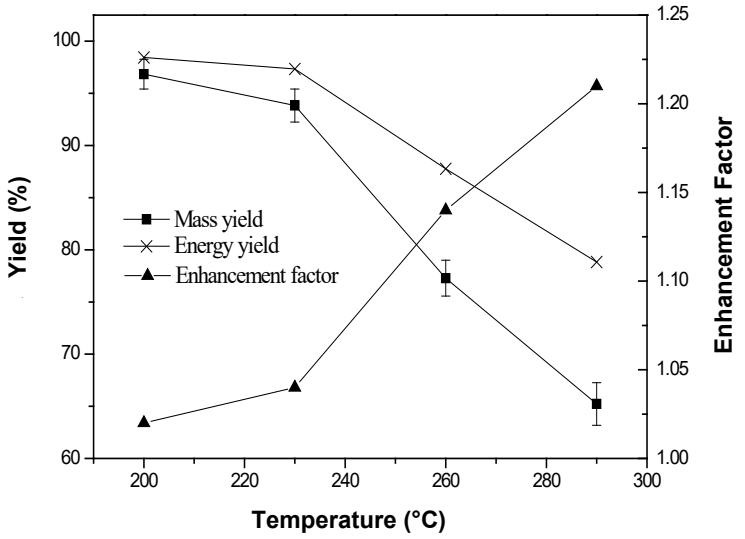

Fig. 1. Mass yield, energy yield and enhancement factor of TPs at different temperatures

It could be seen from Fig. 1 that the energy yield of the TP was consistent with the changing trend of mass yield. When the torrefaction temperature was lower than 230 °C, the decrease of mass yield was not obvious; when the temperature exceeded 230 °C, the mass yield dropped significantly. However, in all experiments under the same conditions, the energy yield was higher than the mass yield. The energy yield represented the total energy retained in the TPs. As the torrefaction temperature increased, the enhancement factor increased. When the torrefaction temperatures were 200, 230, 260, and 290 °C, the enhancement factor of the TP, which could be calculated using the data (enhancement factor curve) in Fig. 1, increased by 2%, 4%, 14%, 21%, respectively, and the growth rate also gradually increased. For high torrefaction temperature, the significant increase in enhancement factor was due to the rapid increase of HHV in samples. However, although a higher HHV value can be obtained when torrefaction was 280 °C, its yield of energy and mass was also relatively low. This showed that although torrefaction can improve the calorific value of the sample that remains after torrefaction, when considering the mass loss, the overall energy value of the sample was reduced. The escape of some flammable volatiles during torrefaction is the main cause of energy loss in the TPs. On the other hand, the energy yield of TPs was obviously higher than that of mass yield, and the variation range was smaller than that of mass yield. This indicated that although there was a loss in the total energy of the TPs, the decrease in the energy yield of the TPs was smaller than the decrease in the mass yield, so that the fuel quality of the biomass can be greatly improved without losing a small amount of energy.

The torrefaction severity index (TSI) was used to analyze and define the degree of weight loss of biomass under different torrefaction conditions, and the formula is as follows:

$$TSI = \frac{WL_{T,t}}{WL_{290℃,60min}} = \frac{100 - SY_{T,t}}{100 - SY_{290℃,60min}} \quad (8)$$

where $WL_{T,t}$ represents the weight loss of the torrefaction biomass at the specific temperature (T) and holding time (t), whereas SY represents the solids yield of biomass subject to torrefaction. TSI is in the range of 0 to 1 based on the previous definition.

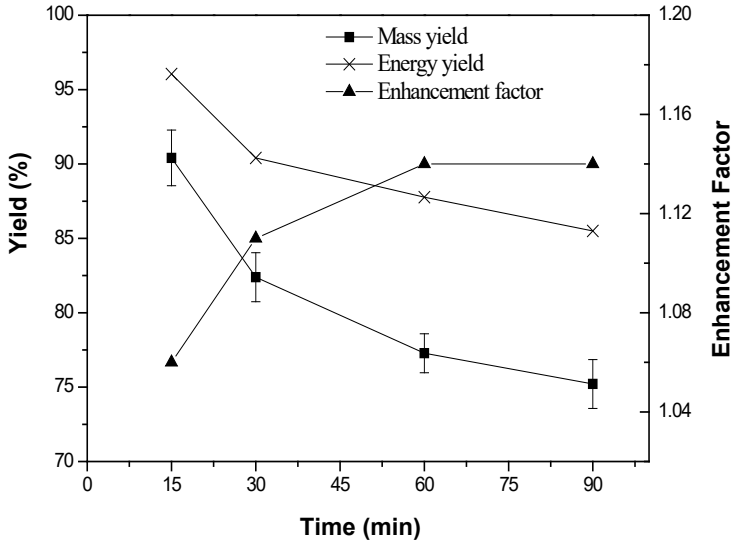

Fig. 2. Effect of TSI (represented here as the time of torrefaction) on energy yield and enhancement factor of torrefaction biomass with different particle sizes

The enhancement factor showed a linear distribution with the TSI, wherein the increase in weight loss would increase the HHV of the torrefaction biomass (Niu *et al.* 2019). The total energy of the biomass tended to decrease with TSI increasing due to the biomass mass loss (Peng *et al.* 2013). The profiles of enhancement factor and energy yield versus TSI are shown in Fig. 2, where regression lines have also been included. The regression lines of energy yield with negative slopes implied that the decreasing degree of solid yield was beyond the increasing degree of the enhancement factor. The slope of the regression lines in Fig. 2 showed that the slope of the regression line of the enhancement factor was 0.21. By contrast, the slopes of regression lines of energy yield were 21.2, implying that the decrease in energy yield was much higher than the increase in HHV. The enhancement factor and energy yield correlated well ($R^2 > 0.99$).

FTIR Spectroscopy

The analysis of FTIR results was conducted by overlapping all the spectra in the same baseline for comparison purposes. Figure 3 shows all FTIR spectra for samples in different torrefaction temperatures. As observed, the trend of the FTIR spectrum of the sample was consistent in different torrefaction temperatures. All spectra showed very broad characteristic peaks at 3410 cm^{-1}, which can be attributed mainly to the weak stretching vibration absorption peaks of –OH groups present in cellulose and hemicellulose. With the deepening of torrefaction degree, the strength of -OH decreased continuously, indicating

that a dehydration reaction had occurred. A characteristic peak appeared at *ca.* 2910 cm^{-1}. That absorbance would indicate C-H stretching vibrations from all of the possible sources in the material. Since the lignin pyrolysis in the sample required a higher temperature, the pyrolysis of lignin did not occur in the torrefaction experiment, so the intensity of this absorption peak did not change significantly.

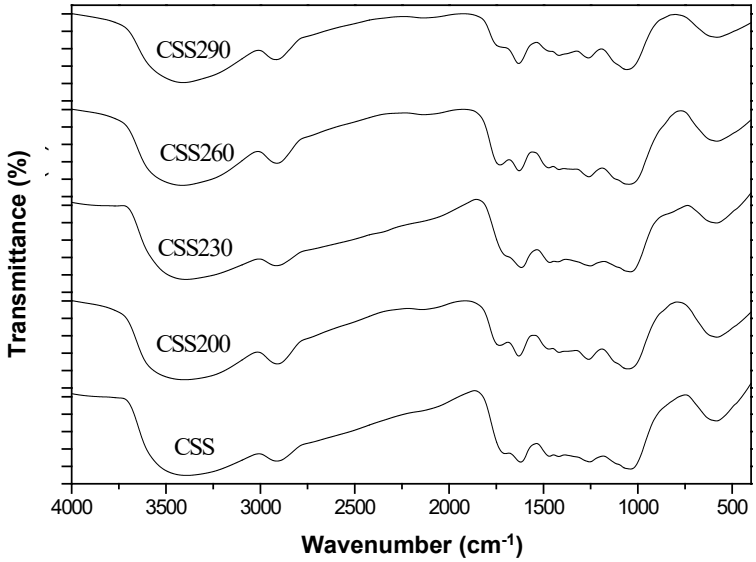

Fig. 3. FTIR spectra for samples in different torrefaction temperatures

The absorption peak near to 1720 cm^{-1} was caused by the C=O stretching vibration on the acetyl group and the carboxyl group, which is a characteristic peak of hemicellulose. For the torrefaction process in an inert atmosphere, different researchers have reported this characteristic peak in detail. In the process of torrefaction deepening, the complete pyrolysis of hemicellulose was caused by deacetylation, resulting in a gradual weakening of the C=O characteristic peak intensity. This behavior depends on the torrefaction process conditions, such as biomass type, particle size, reactor technology, temperature, and residence time (Park *et al.* 2012; Pohlmann *et al.* 2014). The substantial intensity increased at 1620 cm^{-1}, as torrefaction severity increased. This can be ascribed to aromatic skeletal vibrations and guaiacyl ring with CO stretch. An increase in aromatization has been reported in torrefaction under inert atmosphere and was larger when the torrefaction severity increased (Park *et al.* 2013).

Kinetic Analysis of Combustion

As shown in Fig. 4b, the DTA curve of each sample has two distinct peaks, so the combustion of the sample was divided into four stages. The first stage was dehydration. The torrefied sample contained substantially no free water; therefore, this stage was due to the evaporation of crystalline water. The second stage was the separation and combustion of volatile matter. Most of the cellulose and hemicellulose in the sample was decomposed, then separated out as volatile matter and combusted in contact with oxygen. When the volatile components are separated out from sample, a well-developed pore structure will be formed inside, which effectively increases the contact area with oxygen. This stage provides favorable conditions for the ignition of fixed carbon to a certain extent. These changes corresponded to the first peak of the DTG curve. The third stage was the

combustion of fixed carbon. The mass-loss rate in this stage was lower than that in the volatile analysis stage. The reason was that the ash after combustion of the volatile matter enclosed the fixed carbon, which hindered the diffusion of oxygen and slowed the burning rate. This phase corresponded to the second peak of the DTG curve. As the torrefaction temperature increased, the maximum burning rate also increased. This indicated that torrefaction shortened the time of the entire combustion process, which was consistent with the findings of Pala's team (Pala *et al.* 2014). The main mass loss was shifted from the devolatilization and combustion phase (low-temperature zone) to the char combustion phase (high-temperature zone) with the increase in reaction temperature, which was due to the increasing degree of carbonization. The fourth stage was burnout, and there was no further fluctuation in the TG and DTG curves.

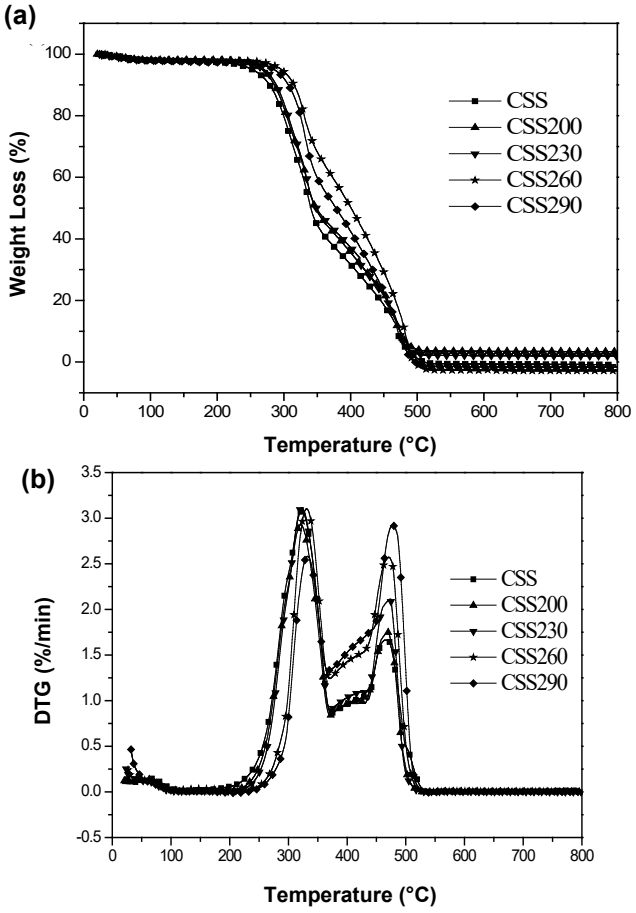

Fig. 4. Combustion characteristics of the sample TG (a) and DTG (b)

Combustion Characteristics Analysis

Mastering the combustion characteristics of fuel is the key to rational utilization of biomass fuel, and also provides basic data for designing or optimizing combustion equipment. In order to understand the application potential of raw materials in combustion before and after roasting, the thermogravimetric method was used to analyze the combustion characteristics in this paper. The combustion characteristic parameters such as the peak temperature and the corresponding mass loss rate (T_{peak} and D_{max}) were calculated based on the literature (Zhang *et al.* 2018b). The ignition and burnout temperatures (T_i and

T_e) of biofuels obtained were evaluated by the intersection method and conversion method. To comprehensively analyze the combustion characteristics of the samples, the experimental results were analyzed using the complete combustion characteristic index (S). The value of S can be calculated according to Eq. 9. The comprehensive combustion characteristic index reflected the ignition characteristics and burnout characteristics of the sample, which is an important parameter, indicating the combustion reaction. The larger the S value was, the better the combustion characteristics of the fuel would be,

$$S = \frac{\left(d_w/d_t\right)_{\max} \cdot \left(d_w/d_t\right)_{mean}}{T_i^2 T_e} \quad (9)$$

where $(\frac{\mathrm{d}w}{\mathrm{d}t})_{max}$ is the maximum burning rate (%/min), $\frac{\mathrm{d}w}{\mathrm{d}t}$ is the average burning rate (%/min), T_e is the burnout temperature (°C), and T_i is the ignition temperature (°C).

The calculation results are shown in Table 2. As the torrefaction temperature increased, the index of the comprehensive combustion characteristics of the sample decreased, indicating that the combustion characteristics of the TP were getting worse. The main reason was that the raw material used in the experiments was seed material. The oil content of the seed material is high. During the roasting process, with the decrease of the oil content, the ignition characteristics will become worse, the burning rate will decrease, and the burnout temperature will increase, and the burning characteristics of TPs will gradually deteriorate.

Table 2. Combustion Characteristics of the Sample

Sample	T_i (°C)	T_e (°C)	T_{peak1} (°C)	D_{max1} (%/min)	T_{peak2} (°C)	D_{max2} (%/min)	D_{mean} (%/min)	S (%^{2}min^{-2}°C^{-3})
CSS	278.9	518.6	322.1	3.08	465.2	1.66	0.57	4.35E-8
CSS200	287.6	528.4	320.9	2.89	469.5	1.75	0.65	4.30E-8
CSS230	294.5	536.5	322.8	3.11	473.6	2.11	0.63	4.21E-8
CSS260	306.9	542.4	331.1	3.10	475.4	2.57	0.59	3.58E-8
CSS290	309.9	548.3	332.6	2.78	478.3	2.92	0.74	4.10E-8

Kinetic Analysis of Combustion

Figure 5 is a relation diagram of $\ln[-\ln(1-x)/T^2]$ and $1/T$. The relationship curve from Fig. 5 is not a simple straight line, which means that the combustion process was not a first-order reaction. This result was consistent with the First Order Pseudo Bi-component Separate-stage Model (PBSM-O1) proposed by Liu *et al.* (2002). The model assumed that the mass loss process of the sample involved three steps. The first step was the evaporation of water, and the two subsequent mass loss steps were mainly due to two major pseudo components. The two-pseudo components were decomposed in two different temperature regions, respectively, other than at the global temperature region as used in the previously developed models by other authors. In the lower and higher temperature ranges, the overall mass loss rate of the sample was controlled by the reaction of the two components, respectively. This process can be described as two consecutive first-order reactions. Therefore, this study referred to the method of Liu *et al.* (2002) to divide the combustion process of the sample into two stages and used PBSM-O1 to carry out kinetic analysis of the whole combustion process.

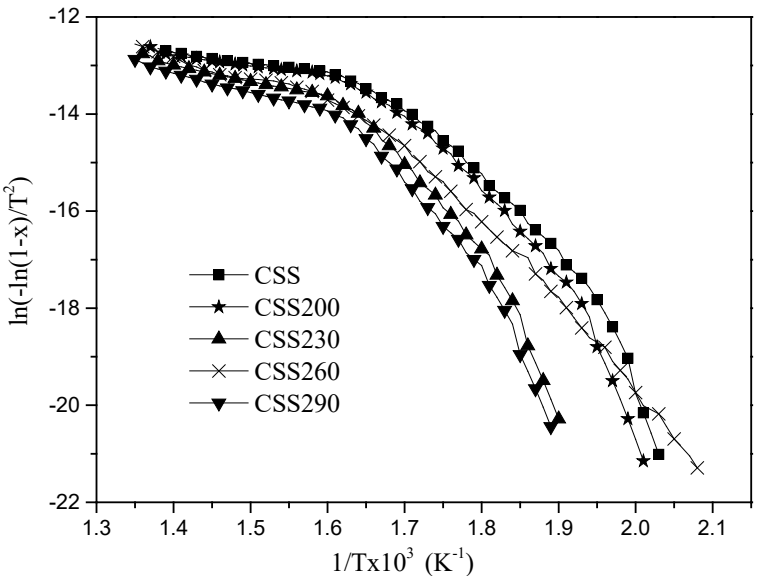

Fig. 5. Plots of ln[-ln(1-*x*)/T^2] vs 1/*T* of TPs.

Table 3 shows the kinetic parameters of all samples determined by this method. The values of the linear coefficients of determination for each sample exceeded 0.9, indicating that the method of describing the combustion process of the raw materials and the TPs with PBSM-O1 was feasible and accurate. Compared with the raw material, the activation energy and pre-exponential factor of the sample at the low-temperature stage increased significantly, and the main reaction temperature region of combustion also shifted to the high temperature. This was mainly due to a large proportion of reactions between cellulose and hemicellulose with lower decomposition temperature during the torrefaction process, and the proportion of lignin with higher decomposition temperature increased. Therefore, the activation energy and the pre-exponential factor of the TPs were significantly improved at this stage. Meantime, the activation energy and pre-exponential factor of the sample in the low-temperature stage were significantly higher than the high-temperature stage.

Table 3. Combustion Kinetic Parameters of Raw Materials and TPs

Sample	Temperature (°C)	*E* (kJ/mol)	*A* (min^{-1})	R^2
CSS	193.9-334.3	116.10	1.96E+10	0.9904
	337.5-448.9	89.92	4.32E+06	0.9488
CSS200	217.7-353.2	143.56	4.01E+12	0.9804
	355.7-469.8	117.97	2.71E+08	0.9717
CSS230	223.4-345.3	155.52	5.11E+13	0.9852
	348.1-453.0	117.11	4.12E+08	0.9795
CSS260	252.8-353.8	194.86	9.45E+16	0.9857
	356.2-470.6	126.51	1.24E+09	0.9418
CSS290	255.6-341.3	214.35	7.55E+18	0.9776
	344.1-446.1	148.45	2.85E+11	0.9815

CONCLUSIONS

Torrefaction is a promising technique in the study of biomass fuel properties. In this study, camellia seed shell (CSS) was torrefied at a temperature of 200 to 290 °C. The effects of torrefaction on the physical properties and combustion kinetics of CSS were investigated. The results showed that the fuel properties of CSS were significantly improved by torrefaction. Torrefaction turned agricultural waste with lower energy content into solid fuel of consistent quality. The torrefaction process increased the activation energy and reaction order of straw burning to different degrees. As the torrefaction temperature increased, the HHV also increased, but the mass and energy yields showed the opposite trends. Compared with CSS290, the HHV of CSS260 was only 1.46 MJ/kg lower, but it had better fuel quality and combustion characteristics. From an economic point of view, the best torrefaction temperature for CSS was 260 °C. Torrefaction was beneficial to the improvement of biomass fuel properties and physicochemical properties; it also had a positive effect on improving the quality of biomass fuels.

ACKNOWLEDGMENTS

The authors wish to acknowledge the financial support under the 2020 Fundamental Research Project of Zhejiang Tongji Vocational College of Science and Technology (FRF20PY001), the Fundamental Research Project of Provincial Universities in Zhejiang (2021XZ009), and the Doctoral Scientific Research Foundation Project of Zhejiang Shuren University entitled 'Research on a Circular Agriculture Model under the Background of Ecological Civilization'.

REFERENCES CITED

Chen, W., and Bach, Q. V. (2017). "A comprehensive study on pyrolysis kinetics of microalgal biomass," *Energy Conversion and Management* 131, 109-116. DOI: 10.1016/j.enconman.2016.10.077

Chen, D., Cen, K., Gan, Z., Zhuang, X., and Ba, Y. (2022). "Comparative study of electric-heating torrefaction and solar-driven torrefaction of biomass: Characterization of property variation and energy usage with torrefaction severity," *Applications in Energy and Combustion Science* 9, article no. 100051. DOI: 10.1016/j.jaecs.2021.100051

Cheng, X., Yang, T., Wang, Y., Zhou, B., Yan, L., Teng, L., Wang, F., Chen, L., He, Y., Guo, K., and Zhang, D. (2018). "New method for effective identification of adulterated camellia oil basing on *Camellia oleifera*-specific DNA," *Arabian Journal of Chemistry* 11(6), 815-826. DOI: 10.1016/j.arabjc.2017.12.025

Dai, L., Wang, Y., Liu, Y., Ruan, R., He, C., Yu, Z., Jiang, L., Zeng, Z., and Tian, X., (2019). "Integrated process of lignocellulosic biomass torrefaction and pyrolysis for upgrading bio-oil production: A state-of-the-art review," *Renewable and Sustainable Energy Reviews* 107, 20-36. DOI: 10.1016/j.rser.2019.02.015

Friedl, A., Padouvas, E., Rotter, H., and Varmuza, K. (2005). "Prediction of heating values of biomass fuel from elemental composition," *Analytica Chimica Acta* 544(1-2), 191-198. DOI: 10.1016/j.aca.2005.01.041

Guo, H., Bi, C., Zeng, C., Ma, W., Yan, L., Li, K., and Wei, K. (2018). "*Camellia oleifera* seed shell carbon as an efficient renewable bio-adsorbent for the adsorption removal of hexavalent chromium and methylene blue from aqueous solution," *Journal of Molecular Liquids* 249, 629-636. DOI: 10.1016/j.molliq.2017.11.096

Hu, Q., Zhang, J., Xing, R., Yu, N., and Chen, Y. (2022). "Integration of lipidomics and metabolomics for the authentication of camellia oil by ultra-performance liquid chromatography quadrupole time-of-flight mass spectrometry coupled with chemometrics," *Food Chemistry* 373, article no. 131534. DOI: 10.1016/j.foodchem.2021.131534

Huang, Y., Cheng, P., Chiueh, P. T., and Lo, S. L. (2017). "Leucaena biochar produced by microwave torrefaction: Fuel properties and energy efficiency," *Applied Energy* 204, 1018-1025. DOI: 10.1016/j.apenergy.2017.03.007

Liang, J., Qu, T., Kun, X., Zhang, Y., Chen, S., Cao, Y., Xie, M., and Guo, X. (2018). "Microwave assisted synthesis of camellia oleifera shell-derived porous carbon with rich oxygen functionalities and superior supercapacitor performance," *Applied Surface Science* 436, 934-940. DOI: 10.1016/j.apsusc.2017.12.142

Liu, N., Fan, W., Dobashi, R., and Huang, L. (2002). "Kinetic modeling of thermal decomposition of natural cellulosic materials in air atmosphere," *Journal of Analytical and Applied Pyrolysis* 63(2), 303-325. DOI: 10.1016/s0165-2370(01)00161-9

Mehmood, M. A., Ye, G., Luo, H., Liu, C., Malik, S., Afzal, I., Xu, J., and Ahmad, M. S. (2017). "Pyrolysis and kinetic analyses of Camel grass (*Cymbopogon schoenanthus*) for bioenergy," *Bioresour Technology* 228, 18-24. DOI: 10.1016/j.biortech.2016.12.096

Niu, Y., Lv, Y., Lei, Y., Liu, S., Liang, Y., Wang, D., and Hui, S. (2019). "Biomass torrefaction: properties, applications, challenges, and economy," *Renewable and Sustainable Energy Reviews* 115, article no. 109395. DOI:10.1016/j.rser.2019.109395

Pala, M., Kantarli, I. C., Buyukisik, H. B., and Yanik, J. (2014). "Hydrothermal carbonization and torrefaction of grape pomace: a comparative evaluation," *Bioresource Technology* 161, 255-262. DOI: 10.1016/j.biortech.2014.03.052

Park, J., Meng, J., Lim, K. H., Rojas, O. J., and Park, S. (2013). "Transformation of lignocellulosic biomass during torrefaction," *Journal of Analytical and Applied Pyrolysis* 100, 199-206. DOI: 10.1016/j.jaap.2012.12.024

Park, S. W., Jang, C., Baek, K.R., and Yang, J. (2012). "Torrefaction and low-temperature carbonization of woody biomass: Evaluation of fuel characteristics of the products," *Energy*, *45*(1), 676-685. DOI: 10.1016/j.energy.2012.07.024

Peng, J., Bi, X., Sokhansanj, S., and Lim, C. J. (2013). "Torrefaction and densification of different species of softwood residues," *Fuel* 111, 411-421. DOI: 10.1016/j.fuel.2013.04.048

Pohlmann, J. G., Osório, E., Vilela, A. C. F., Diez, M. A., and Borrego, A. G. (2014). "Integrating physicochemical information to follow the transformations of biomass upon torrefaction and low-temperature carbonization," *Fuel* 131, 17-27. DOI: 10.1016/j.fuel.2014.04.067

Sarker, R. T., Azargohar, R., Dalai A. K., and Meda, V. (2021). "Enhancement of fuel and physicochemical properties of canola residues *via* microwave torrefaction," *Energy Reports* 7, 6338-6353. DOI: 10.1016/j.egyr.2021.09.068

Tian, X., Dai, L., Wang, Y., Zeng, Z., Zhang, S., Jiang, L., Yang, X., Yue, L., Liu, Y., and Ruan, R. (2020). "Influence of torrefaction pretreatment on corncobs: A study on

fundamental characteristics, thermal behavior, and kinetic," *Bioresource Technology*, 297, article no. 122490. DOI: 10.1016/j.biortech.2019.122490

Xin, S., Mi, T., Liu, X., and Huang, F. (2018). "Effect of torrefaction on the pyrolysis characteristics of high moisture herbaceous residues," *Energy* 152, 586-593. DOI: 10.1016/j.energy.2018.03.104

Zhang, J., Gong, L., Sun, K., Jiang, J., and Zhang, X. (2012). "Preparation of activated carbon from waste *Camellia oleifera* shell for supercapacitor application," *Journal of Solid State Electrochemistry* 16(6), 2179-2186. DOI: 10.1007/s10008-012-1639-1

Zhang, C., Ho, S. H., Chen, W., Xie, Y., Liu, Z., and Chang, J. (2018a). "Torrefaction performance and energy usage of biomass wastes and their correlations with torrefaction severity index," *Applied Energy* 220, 598-604. DOI: 10.1016/j.apenergy.2018.03.129

Zhang, S., Su, Y., Xu, D., Zhu, S., Zhang, H., and Liu, X. (2018b). "Assessment of hydrothermal carbonization and coupling washing with torrefaction of bamboo sawdust for biofuels production," *Bioresource Technology* 258, 111-118. DOI: 10.1016/j.biortech.2018.02.127

Article submitted: January 24, 2022; Peer review completed: April 30, 2022; Revised version received and accepted: May 7, 2022; Published: May 13, 2022.
DOI: 10.15376/biores.17.3.4055-4068